Effective 3D viscoelasticity of red blood cells measured by diffraction phase microscopy

Ru Wang,[1] Huafeng Ding,[1] Mustafa Mir,[1] Krishnarao Tangella,[2] and Gabriel Popescu[1,*]

[1]*Quantitative Light Imaging Laboratory, Department of Electrical and Computer Engineering, Beckman Institute for Advanced Science and Technology, University of Illinois at Urbana-Champaign, Urbana. IL 61801, USA*

[2]*Department of Pathology, Christie Clinic and University of Illinois at Urbana-Champaign, Urbana, IL, 61801, USA*

**gpopescu@illinois.edu*

Abstract: We present optical measurements of nanoscale red blood cell fluctuations obtained by highly sensitive quantitative phase imaging. These spatio-temporal fluctuations are modeled in terms of the bulk viscoelastic response of the cell. Relating the displacement distribution to the storage and loss moduli of the bulk has the advantage of incorporating all geometric and cortical effects into a single effective medium behavior. The results on normal cells indicate that the viscous modulus is much larger than the elastic one throughout the entire frequency range covered by the measurement, indicating fluid behavior.

OCIS codes: (000.0000) General; (000.2700) General science.

References and links

1. N. Mohandas, and P. G. Gallagher, "Red cell membrane: past, present, and future," Blood **112**(10), 3939–3948 (2008).
2. R. Cotran, V. Kumar, T. Collins, and S. Robbins, *Robbins Pathologic Basis of Disease* (WB Saunders Company, 2004).
3. G. Bao, and S. Suresh, "Cell and molecular mechanics of biological materials," Nat. Mater. **2**(11), 715–725 (2003).
4. D. E. Discher, N. Mohandas, and E. A. Evans, "Molecular maps of red cell deformation: hidden elasticity and in situ connectivity," Science **266**(5187), 1032–1035 (1994).
5. H. Engelhardt, H. Gaub, and E. Sackmann, "Viscoelastic properties of erythrocyte membranes in high-frequency electric fields," Nature **307**(5949), 378–380 (1984).
6. M. Dao, C. T. Lim, and S. Suresh, "Mechanics of the human red blood cell deformed by optical tweezers," J. Mech. Phys. Solids **51**(11-12), 2259–2280 (2003).
7. J. Sleep, D. Wilson, R. Simmons, and W. Gratzer, "Elasticity of the red cell membrane and its relation to hemolytic disorders: an optical tweezers study," Biophys. J. **77**(6), 3085–3095 (1999).
8. M. Puig-de-Morales, K. T. Turner, J. P. Butler, J. J. Fredberg, and S. Suresh, "Viscoelasticity of the human red blood cell," J. Appl. Physiol. **293**, 597–605 (2007).
9. M. S. Amin, Y. K. Park, N. Lue, R. R. Dasari, K. Badizadegan, M. S. Feld, and G. Popescu, "Microrheology of red blood cell membranes using dynamic scattering microscopy," Opt. Express **15**(25), 17001–17009 (2007).
10. F. Brochard, and J. F. Lennon, "Frequency spectrum of the flicker phenomenon in erythrocytes," J. Phys. **36**, 1035–1047 (1975).
11. S. Levin, and R. Korenstein, "Membrane fluctuations in erythrocytes are linked to MgATP-dependent dynamic assembly of the membrane skeleton," Biophys. J. **60**(3), 733–737 (1991).
12. D. H. Boal, U. Seifert, and A. Zilker, "Dual network model for red blood cell membranes," Phys. Rev. Lett. **69**(23), 3405–3408 (1992).
13. S. Tuvia, S. Levin, and R. Korenstein, "Correlation between local cell membrane displacements and filterability of human red blood cells," FEBS Lett. **304**(1), 32–36 (1992).
14. S. Tuvia, A. Almagor, A. Bitler, S. Levin, R. Korenstein, and S. Yedgar, "Cell membrane fluctuations are regulated by medium macroviscosity: evidence for a metabolic driving force," Proc. Natl. Acad. Sci. U.S.A. **94**(10), 5045–5049 (1997).
15. N. Gov, A. G. Zilman, and S. Safran, "Cytoskeleton confinement and tension of red blood cell membranes," Phys. Rev. Lett. **90**(22), 228101 (2003).
16. N. Gov, "Membrane undulations driven by force fluctuations of active proteins," Phys. Rev. Lett. **93**(26), 268104 (2004).
17. L. C. L. Lin, and F. L. H. Brown, "Brownian dynamics in Fourier space: membrane simulations over long length and time scales," Phys. Rev. Lett. **93**(25), 256001 (2004).
18. G. Popescu, T. Ikeda, K. Goda, C. A. Best-Popescu, M. Laposata, S. Manley, R. R. Dasari, K. Badizadegan, and M. S. Feld, "Optical measurement of cell membrane tension," Phys. Rev. Lett. **97**(21), 218101 (2006).

#139052 - $15.00 USD Received 2 Dec 2010; revised 7 Jan 2011; accepted 29 Jan 2011; published 3 Feb 2011

19. L. C. L. Lin, N. Gov, and F. L. H. Brown, "Nonequilibrium membrane fluctuations driven by active proteins," J. Chem. Phys. **124**(7), 074903 (2006).
20. Y. K. Park, M. Diez-Silva, G. Popescu, G. Lykotrafitis, W. Choi, M. S. Feld, and S. Suresh, "Refractive index maps and membrane dynamics of human red blood cells parasitized by *Plasmodium falciparum*," Proc. Natl. Acad. Sci. U.S.A. **105**(37), 13730–13735 (2008).
21. N. S. Gov, and S. A. Safran, "Red blood cell membrane fluctuations and shape controlled by ATP-induced cytoskeletal defects," Biophys. J. **88**(3), 1859–1874 (2005).
22. R. Lipowsky, and M. Girardet, "Shape fluctuations of polymerized or solidlike membranes," Phys. Rev. Lett. **65**(23), 2893–2896 (1990).
23. A. J. Levine, and F. C. MacKintosh, "Dynamics of viscoelastic membranes," Phys. Rev. E Stat. Nonlin. Soft Matter Phys. **66**(6), 061606 (2002).
24. Y. K. Park, C. A. Best, T. Auth, N. S. Gov, S. A. Safran, G. Popescu, S. Suresh, and M. S. Feld, "Metabolic remodeling of the human red blood cell membrane," Proc. Natl. Acad. Sci. U.S.A. **107**(4), 1289–1294 (2010).
25. M. A. Peterson, "Geometrical methods for the elasticity theory of membranes," J. Math. Phys. **26**(4), 711–717 (1985).
26. G. Popescu, "Quantitative phase imaging of nanoscale cell structure and dynamics.methods in cell biology." in *Methods in Nano Cell Biology*, B. P.Jena, ed. (Elsevier. 2008) pp. 87–115.
27. T. G. Mason, and D. A. Weitz, "Optical measurements of frequency-dependent linear viscoelastic moduli of complex fluids," Phys. Rev. Lett. **74**(7), 1250–1253 (1995).
28. J. D. Wan, W. D. Ristenpart, and H. A. Stone, "Dynamics of shear-induced ATP release from red blood cells," Proc. Natl. Acad. Sci. U.S.A. **105**(43), 16432–16437 (2008).
29. G. Popescu, T. Ikeda, R. R. Dasari, and M. S. Feld, "Diffraction phase microscopy for quantifying cell structure and dynamics," Opt. Lett. **31**(6), 775–777 (2006).
30. N. Gov, A. Zilman, and S. Safran, "Cytoskeleton confinement of red blood cell membrane fluctuations," Biophys. J. **84**, 486A (2003).
31. A. G. Zilman, and R. Granek, "Undulations and dynamic structure factor of membranes," Phys. Rev. Lett. **77**(23), 4788–4791 (1996).
32. G. Popescu, A. Dogariu, and R. Rajagopalan, "Spatially resolved microrheology using localized coherence volumes," Phys. Rev. E Stat. Nonlin. Soft Matter Phys. **65**(4), 041504 (2002).
33. H. Ding, Z. Wang, F. Nguyen, S. A. Boppart, and G. Popescu, "Fourier transform light scattering of inhomogeneous and dynamic structures," Phys. Rev. Lett. **101**(23), 238102 (2008).
34. H. Ding, L. J. Millet, M. U. Gillette, and G. Popescu, "Actin-driven cell dynamics probed by Fourier transform light scattering," Biomed. Opt. Express **1**(1), 260–267 (2010).
35. D. Langevin, *Light Scattering by Liquid Surfaces and Complementary Techniques* (M. Dekker, New York, 1992).
36. Y. C. Fung, *Biomechanics: Mechanical Properties of Living Tissues* (Springer-Verlag, New York, 1993).
37. F. Gittes, and F. C. MacKintosh, "Dynamic shear modulus of a semiflexible polymer network," Phys. Rev. E Stat. Phys. Plasmas Fluids Relat. Interdiscip. Topics **58**(2), R1241–R1244 (1998).

1. Introduction

The red blood cell (RBC) deformability in microvasculature governs the cell's ability to transport oxygen in the body [1]. Interestingly, RBCs must pass periodically a deformability test by being forced to squeeze through narrow passages (sinuses) in the spleen; upon failing this mechanical assessment, the cell is destroyed and removed from circulation by macrophages (a type of white cell) [2]. Thus, understanding the microrheology of RBCs is highly interesting both from a basic science and clinical practice point of view.

However, the mechanics of this system is insufficiently understood. A number of different techniques have been previously used to study the rheology of live cells [3]. Among these, pipette aspiration [4], electric field deformation [5], and optical tweezers [6,7] provide quantitative information about the shear and bending moduli of RBC membranes. Dynamic, frequency-dependent knowledge of the RBC mechanical response has been limited to recent developments based on active and passive microbead rheology [8,9].

RBC membrane thermal fluctuations have been studied intensively, as they offer a non-perturbing window into the structure, dynamics, and function of the whole cell [10–20]. These spontaneous motions have been modeled theoretically under both static and dynamic conditions to connect the statistics of the membrane displacements to relevant mechanical properties of the cell [10,15,16,21–23]. With few exceptions [24,25], all membrane models assume a flat, 2D cell surface.

Here we present quantitative optical measurements of RBC fluctuations obtained by highly sensitive quantitative phase imaging [26]. These spatio-temporal fluctuations are modeled in terms of the bulk viscoelastic response of the cell, which carries the spirit of the

#139052 - $15.00 USD Received 2 Dec 2010; revised 7 Jan 2011; accepted 29 Jan 2011; published 3 Feb 2011

passive microrheology method pioneered by Mason and Weitz [27]. Relating the displacement distribution to the storage and loss moduli of the bulk has the advantage of incorporating all geometric and cortical effects into a single effective medium behavior. Essentially, we treat the cell as a viscoelastic droplet that recovers the 3D shear behavior of the cell as it exhibits itself in flow [28].

2. Experimental setup

The experimental setup is a modified version of the diffraction phase microscope (DPM), which is described in more detail elsewhere [29]. Briefly, using laser illumination and a common path interferometer, we generate an extremely stable interferogram at the image plane of a transmission microscope. The final quantitative phase image is obtained from this interferogram using a Hilbert transform. Red blood cells from a healthy volunteer were imaged at a rate of 20 frames/s and the phase shift information $\phi(x, y)$ was translated into cell thickness distribution h(x, y) using $h = \phi\lambda / 2\pi(n - n_0)$, with λ = 532 nm the laser wavelength, n = 1.41 the refractive index of the hemoglobin, and n_0 = 1.34 the refractive index of plasma.

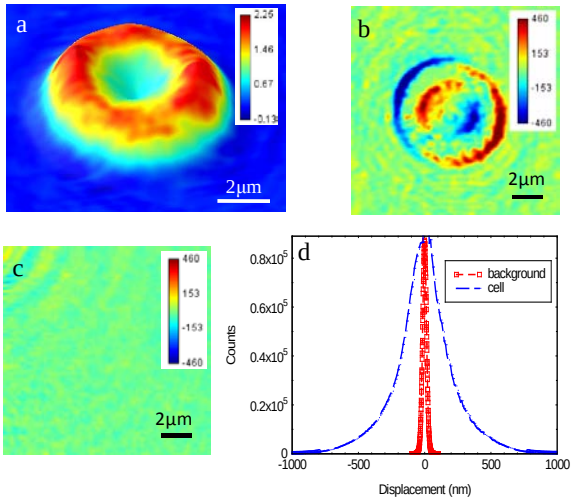

Fig. 1. a) RBC topography map; color bar indicates thickness in microns. b) Instant displacement map; color bar in nm. c) Background displacement; color bar in nm. d) Histogram of displacements associated with the mps in b and c.

Figure 1a shows an RBC thickness distribution, $\bar{h}(x, y)$, which is the result of averaging 256 frames. A displacement map at an arbitrary moment t $\Delta h(x, y; t) = h(x, y; t) - \bar{h}(x, y)$ is illustrated in Fig. 1b and the background noise in Fig. 1c. Figure 1d shows the histogram of displacements for both the signal (membrane) and noise, which demonstrates the ability of DPM to retrieve membrane fluctuations with high signal to noise ratio. This noise is primarily due to possible fluctuations from the plasma outside the RBC membrane and residual uncommon path vibrations and air fluctuations in the interferometer. The spatially-averaged power spectra, $P(\omega) = \int \Delta h^2(x, y; \omega) dxdy$, for a group of normal RBCs, is illustrated in Fig. 2a. All measured P(ω) curves exhibit power law behavior $\omega^{-\alpha}$ with different exponent values, $\alpha = 1.69 \pm 0.29$ ($\alpha_{\min} = 1.16$ and $\alpha_{\max} = 2.07$) where the error captures the cell-to-cell variability (N = 7). Note that the power law predicted by 2D membrane models, assuming elastic parameters constant frequency, predict narrow values of the exponent $\alpha = 4/3$ [10,30] or $\alpha = 5/3$ [23,31]. Of course, our average exponent, 1.7, is compatible with the 5/3 value. The large variability measured in the power laws, $1 < \alpha < 2$, cannot be easily explained by the

#139052 - $15.00 USD Received 2 Dec 2010; revised 7 Jan 2011; accepted 29 Jan 2011; published 3 Feb 2011

2D, frequency-independent models. However, this power law dependence is in striking resemblance with what has been measured via dynamic light scattering on beads embedded in complex fluids [27,32]. There, it was found that the power spectrum of the scattered light for a purely viscous fluid exhibits ω^{-2} dependence and progressively broadens (i.e. exhibits lower exponents) as the elasticity increases. Our RBC imaging measurements are indeed equivalent to scattering experiments, where the signals are due to the interaction of light with the undulating cell surface [33]. This merger of scattering and imaging measurements is possible due to the knowledge of phase at each point in the image plane, which allows for numerically propagating the complex optical field at any arbitrary plane in space, including the far-field (i.e., scattering plane) [33]. This new approach, referred to as Fourier Transform Light Scattering, provides extremely sensitive and fast scattering measurements, which recently allowed the non-contact probing of actin-mediated nanoscale membrane motions in live cells [34].

3. Theory

We modeled the cell as a homogeneous droplet that undergoes surface fluctuations at thermal equilibrium. In analogy to scattering-based microrheology, this viscous response, which relates to the measured power spectrum via the fluctuation dissipation theorem, is later generalized to include elasticity. The general solution of a liquid surface fluctuations under thermal equilibrium conditions is due to Bouchiat and described in more detail in [35],

$$\Delta h^2(q,\omega) = -\frac{k_B T}{\pi\omega}\frac{q\tau_0^2}{\rho}\mathrm{Im}\left(\frac{1}{\beta+(1+\alpha)^2-\sqrt{1+2\alpha}}\right)\Big|_{\alpha=i\omega\tau_0} \quad (1)$$

where $\beta = \sigma\rho/4\eta^2 q$, $\tau_0 = \rho/2\eta q^2$, q is the wave number (0.1-1 μm^{-1}), ρ is the cytosol density ($\rho \simeq 1.5 kg/m^3$), η the cytosol viscosity ($\eta \simeq 6\cdot 10^{-3}\ Pa\cdot s$) [36]and σ the surface tension ($\sigma \simeq 10^{-6}\ N/m$) [29]. Due to the low surface tension associated with RBCs and high spatial frequencies probed in our experiments, Eq. (1) reduces to

$$\Delta h^2(q,\omega) \simeq \frac{k_B T}{2\pi q\omega^2}\frac{1}{\eta(\omega)} \quad (2)$$

Note that, for a purely viscous cell, i.e. $\eta = constant$, the fluctuation spectrum recovers the expected ω^{-2} behavior. Using the fluctuation dissipation theorem, the viscous response function can be written as

$$\chi''(q,\omega) = \frac{\pi\omega}{k_B T}\Delta h^2(q,\omega) \quad (3)$$

The real (elastic) part of the response is obtained via the Kramers-Kronig relationship

$$\overline{\chi}'(\omega) = \frac{2}{\pi}P\int_{-\infty}^{+\infty}\frac{\overline{\chi}''(\omega')}{\omega'-\omega}d\omega', \quad (4)$$

In Eq. (4), P indicates the principal value integral and the spatial dependence of χ'' was averaged out, i.e. $\overline{\chi}''(\omega) = 2\pi\int\chi''(q,\omega)qdq$. In order to calculate the Hilbert transform in Eq. (4), we used the best fit of P(ω) (see Fig. 2) with a power law function instead of the actual data. This approach minimizes the effect of noise in evaluating the integral of Eq. (3), as previously described in Ref [27].

#139052 - $15.00 USD Received 2 Dec 2010; revised 7 Jan 2011; accepted 29 Jan 2011; published 3 Feb 2011

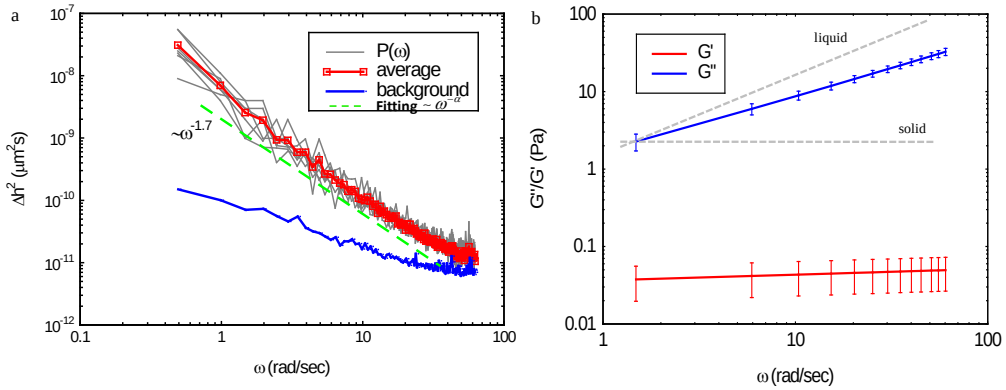

Fig. 2. (a) Power spectra of membrane fluctuations for 7 RBCs, their average, and background, as indicated. Dash line indicates a power law of exponent –1.7. (b). RBC viscous and elastic moduli vs. frequency, as indicated. Dash lines show the liquid and solid behavior.

The viscoelastic modulus was obtained by using its proportionality with the complex, frequency dependent viscosity, $G^* = i\omega\eta^*$. Figure 2(b) summarizes the results in terms of the viscous modulus, G"(ω), and elastic modulus, G'(ω), for a set of 7 RBCs. As expected, the loss modulus G" is dominant, which indicates a largely fluid behavior of the normal cell. The loss modulus G" has a power law dependence on frequency with and exponent between 1 and 2, as expected for a viscoelastic fluid. This behavior agrees qualitatively with that reported by Puig-de-Morales et al. [8], where the magnetic bead twisting method was employed to retrieve the 2D viscoelastic moduli of the cell membrane.

4. Discussion

In the following we discuss the physical interpretation of our experimental results. The treatment of the RBC as a viscoelastic droplet originated in the experimental observation that the power spectra measured in our experiments on RBCs have the same characteristics as those measured by dynamic light scattering microrheology. These power spectra become continuously broader for stiffer cells, which cannot be accounted for by previous membrane models, which predict a fixed power law. Thus it appears that RBC flickering can be interpreted as due to the 3D shear response of a viscoelastic medium. In the bead microrheology, the relationship between the complex response function and shear modulus is obtained via the generalized Stokes-Einstein equation (GSER)

$$G(\omega)_{GSER} = \frac{1}{6\pi a}\frac{1}{\chi(\omega)}, \qquad (5)$$

where a is the radius of the probing bead.. In the RBC case, the analog relationship is obtained, up to a constant, by replacing a with the 1/q. We emphasize that the physical origin of this equivalence is not entirely clear. We propose a picture that may provide a heuristic explanation for these observations. Figure 3 depicts the instantaneous displacement map associated with a discocyte. The spatial contributions from the spatial wavelength Λ = 1 μm is shown in Fig. 3a. Our results suggest that the surface ripples of a certain (spatial) period, $\Lambda = 2\pi / q$, are equivalent to deformations produced by a spherical bead to a 3D fluid. This is illustrated in

#139052 - $15.00 USD Received 2 Dec 2010; revised 7 Jan 2011; accepted 29 Jan 2011; published 3 Feb 2011

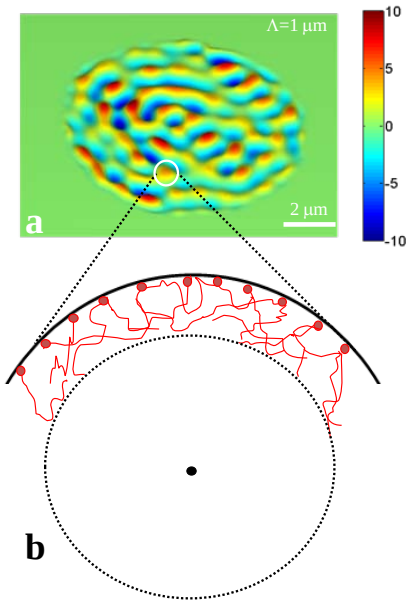

Fig. 3. Instantaneous displacement map associated with an RBC at a spatial wavelength, $\Lambda = 2\pi/q$, centered around 1 μm. Color bar in nanometers indicates displacements in nanometers. b) Schematics of how the membrane ripples deform the membrane material like a bead of size comparable with Λ. The spectrin molecules are depicted in red and connected to the lipid bilayer.

Figure 3b, where the 3D nature of the problem is emphasized by considering a finite thickness of the deformed medium. This picture may explain why the complex modulus G obtained from our data captures the 3D dynamic behavior. It is known that the cytoskeleton is solely responsible for the finite shear resistance of the RBCs in circulation [24]. It is, therefore, not surprising that the frequency dependence of G' and G" are in qualitative agreement with passive microrheology data obtained from polymer solutions [27]. Quantitatively, we always measured lower values for both G' and G" than those reported for actin solutions [27,37] which is expected, as the spectrin filaments are known to be more flexible than the actin ones.

5. Conclusion

In sum, our sensitive measurements of RBC membrane displacements indicate that the dynamics can be accounted for by applying a model of light scattering on fluid surfaces. From the power spectrum of the fluctuations, we can extract the 3D viscoelastic response of the cells and their effective shear moduli. The ability to account for a global descriptor of cell dynamics that explains the measurements without relying on a priori knowledge about the bilayer and spectrin composition may prove useful for high-throughput clinical applications such as blood screening.

Acknowledgments

This research was supported in part by the National Science Foundation (CAREER 08-46660) and the National Cancer Institute (R21 CA147967-01).

#139052 - $15.00 USD Received 2 Dec 2010; revised 7 Jan 2011; accepted 29 Jan 2011; published 3 Feb 2011